Nonlinear Flight Control Design via Sliding Methods

J. Karl Hedrick* and Swaminathan Gopalswamy†
University of California, Berkeley, Berkeley, California 94720

Nonlinear inversion/sliding control techniques are applied to design a pitch axis control system for high-performance aircraft. The control objectives are to track pilot *g* commands while satisfying flying quality specifications. In the pitch axis problem, the dominant nonlinearities are the aerodynamic coefficients variation with angle of attack and saturation of the actuators position and rate response. Two design approaches are investigated; the first defines a single output to be controlled (pilot's normal acceleration) and coordinates the elevator and the flaperon as a single input. The nonminimum phase nature of the resulting input/output pair necessitates defining a modified output to avoid stability problems inherent in inversion methods. The second approach defines a two input/two output problem and directly incorporates the flying quality specifications into the output definition. These two methods are illustrated using a simulation model. The latter approach is shown to allow more freedom to avoid actuator saturation at high *g* commands.

I. Introduction

THE dynamics of high-performance aircraft are highly nonlinear, and therefore control system designs are severely limited by the necessity to linearize and decouple the equations of motion in the development of state-space models. The objective of ongoing research is to develop nonlinear control designs that provide improved performance and reduce development time. In this paper, the application of nonlinear inversion techniques for pitch axis control of a high-performance aircraft are discussed.

Conventional control designs are developed by assuming that the system is at a specific operating point and by approximating the system's response by linear perturbation equations. In addition, longitudinal motion is assumed to be independent of lateral motion, and therefore the equations can be uncoupled and treated independently. This approach allows the application of well-known linear control theory and analytic methods to provide insights into the early design phases. The assumptions are valid only for commands that cause small deviations from the defined operating point. Therefore multiple linear designs are accomplished at selected points in the flight envelope. If the design points are closely spaced, system operation at "off" design conditions can be adequately approximated by linear interpolations between the existing point designs. Thus, the multiple point designs can be collapsed into gain scheduling within the linear design structure.

For high performance aircraft, this approach yields only a starting point for the designer. A significant amount of pilot-in-the-loop simulations must be conducted using high fidelity nonlinear aerodynamic models to reach a realistic design. Control system nonlinearities are added, and simulations with actual flight hardware are accomplished prior to a final design. This is an expensive and time-consuming process requiring multiple redesign efforts. In the process the original linearly developed gains and bandwidths are almost always altered, with an attendant loss in *expected* performance. The most significant areas requiring redesign activities include high angle of attack nonlinearities, nonlinear actuator-surface responses due to actuator rate limiting and surface saturation, and cross-axis kinematic and velocity coupling in the equations of motion.

There has been previous work involving the use of nonlinear techniques for flight control. To mention a few, Garrard and Jordan[1] used a nonlinear optimal control approach to the control of the pitch axis dynamics. Meyer et al.[2] used nonlinear transformations to achieve linearization of the aircraft dynamics. Lane and Stengel[3] designed a controller that "decouples specific state variables that are of particular interest to the pilot" by the use of nonlinear inverse dynamics. Recently, Elgersma and Morton[4] used a controller based on "partial dynamic inversion." They computed the inverse dynamics of as much of the nonlinear system as possible, "then studied the stability of the uninverted part of the system." These works concentrated on obtaining the inverse dynamics of the system to control the outputs.

Two main problems arise in this context—the problem of the zerodynamics and that of actuator saturation. Hauser et al.[5] have used an "approximate linearization technique" to handle the "slightly nonminimum phase" nature of VSTOL aircraft dynamics. The undesirable zerodynamics is a typical problem encountered in aircraft dynamics. Lane and Stengel[3] avoid it by neglecting the forces generated by the control surfaces. Lane and Stengel[3] also present a way of handling actuator saturation in the context of command variable independence. Recently, Kapasouris et al.[6] have dealt with saturation explicitly in linear systems by adjusting the desired trajectories in a smooth manner.

Finally, the problem of robustness of the performance to model errors and disturbances has not been discussed in detail in most of these papers using inverse dynamics. White et al.[7] applied the sliding mode control method to the lateral dynamics of an aircraft, but they do not explicitly deal with the sliding gains that ensure robustness properties.

In this paper, it is shown how the angle of attack nonlinearities present in the aerodynamic coefficients can be directly incorporated into the controller design using inversion techniques, and how the performance can be made robust to model errors by employing sliding controllers. We present a methodology for treating undesirable zerodynamics and present a method for incorporating the flying quality specifications directly into the design.

The objective is to achieve high *g* commands (normal load felt by the pilot) while satisfying flying quality specifications. The flying quality is determined from the specifications on *two* independent variables (related to the normal acceleration and the pitch rate).

Two interesting design approaches are discussed based on nonlinear inversion—a single sliding surface design and a dual sliding surface design. In the first case, the output is the number of *g* pulled, and the inputs are the elevator and the

Received Oct. 3, 1989; revision received March 6, 1990.

*Professor of Mechanical Engineering.
†Graduate Student, Department of Mechanical Engineering.

flaperon. Direct inversion gives excellent tracking but leads to oscillatory behavior of the other states. Therefore an output redefinition approach is used. Thus, tracking and flying quality specifications are satisfied by specifying the auxiliary dynamics through output redefinition. Another important idea involved in this design is that the redundancy in the inputs is taken advantage of in reducing the angle of attack.

In the dual sliding surface design, flying quality specifications are satisfied directly by using the variables for which the specifications are given as the variables to be tracked.

II. Aircraft Model

The aircraft is modeled as a rigid body subjected to aerodynamic and actuator forces. The longitudinal speed of the aircraft u is assumed to remain constant during the pitch axis maneuver; it is assumed that this is achieved by continuous adjustment of the throttle. The dynamic equations are expressed in a body-fixed reference frame. The simplified dynamic equations are

$$\dot{w} = qu + g\cos(\theta) - \left[L\cos(\alpha) + D\sin(\alpha)\right]/m \tag{1}$$

$$\dot{q} = M/Iyy \tag{2}$$

$$\dot{\theta} = q \tag{3}$$

The aerodynamic forces are given by

$$L = \bar{q}S\left[C_{l0} + C_{l\alpha}(\alpha)\alpha + C_{lq}(\alpha)(\bar{c}/2V_t)q + C_{l\delta_e}\delta_e + C_{l\delta_f}\delta_f\right] \tag{4}$$

$$D = \bar{q}S(C_{d0} + C_{d\alpha}\alpha + C_{d\delta_e}\delta_e + C_{d\delta_f}\delta_f) \tag{5}$$

$$M = \bar{q}S\bar{c}\left[C_{m0} + C_{m\alpha}(\alpha)\alpha + C_{mq}(\alpha)(\bar{c}/2V_t)q + C_{m\delta_e}\delta_e + C_{m\delta_f}\delta_f\right] \tag{6}$$

where δ_e and δ_f are the elevator and flaperon angles and

$$\bar{q} = \tfrac{1}{2}\rho V_t^2 \tag{7}$$

$$V_t = \sqrt{u^2 + w^2} \tag{8}$$

$$\tan\alpha = w/u \tag{9}$$

The u is the velocity of the aircraft along the body x axis, w the velocity of the aircraft along the body z axis, and q the angular velocity of the aircraft about the body y axis. The θ is the angle of the flight path (total velocity) with respect to the horizontal, and α is the angle between the total relative velocity and the body x axis. The mass and pitch moment of inertia are m and I_{yy}, respectively.

The actuator dynamics are modeled as

$$\dot{\delta}_e = 20(u_{\delta_e} - \delta_e) \tag{10}$$

$$\dot{\delta}_f = 20(u_{\delta_f} - \delta_f) \tag{11}$$

This modeling neglects higher-order dynamics from the commanded inputs $u^*_{\delta_e}$, $u^*_{\delta_f}$ to the actual inputs u_{δ_e}, u_{δ_f}, which is given by the following transfer function

$$\frac{52^2}{s^2 + (2)(0.7)(52)s + 52^2}$$

In addition to the nonlinearities seen in the coupling terms in the equations of motion, the aerodynamic coefficients are functions of the angle of attack. Figure 1 shows the functions used in this paper. (A real aircraft would not have the sharp breaks shown in Fig. 1.) The actuator saturation effects considered in this paper are given in Table 1.

Table 1 Acutator saturation levels

Surface	Maximum angle, deg	Maximum rate, deg/s
Elevator	25	60
Flaperons	20	52

A. The *g* Command

An important maneuver is the fast pull up, and it is usually translated as a g command. Specifically, the command is for the aircraft to experience a desired normal load factor (NFL) A_n. This is the normalized force required along the normal axis (in the body frame) to keep a unit mass moving with the aircraft at some specified location in the aircraft. The normalization is with respect to the weight of the unit mass. The NLF at two relevant locations of interest are those at the pilot station A_{np} and at the center of gravity A_{ncg}. In this paper, the NLF at the pilot station was chosen for tracking. This is consistent with the specifications given for evaluating handling qualities of the controller as seen by the pilot.

$$A_{ncg} = \left[L\cos(\alpha) + D\sin(\alpha)\right]/(mg) \tag{12}$$

Or,

$$A_{ncg} = -\dot{w}/g + qu/q + \cos\theta \tag{13}$$

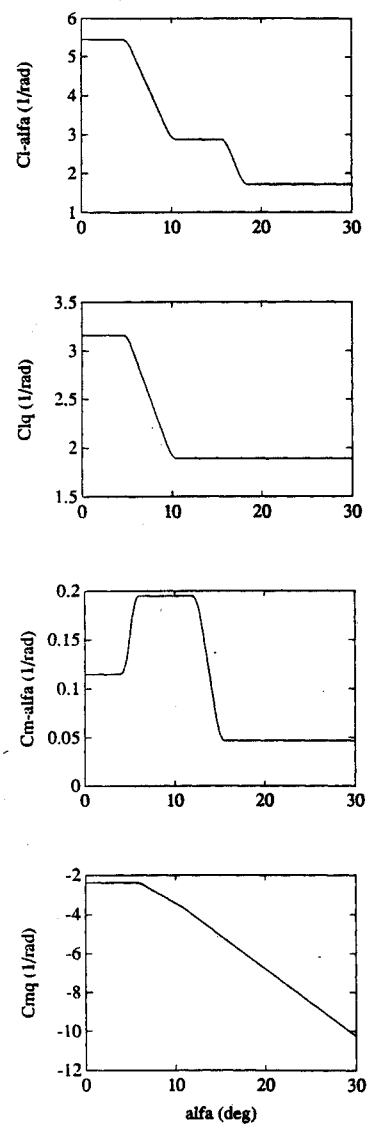

Fig. 1 Aerodynamic nonlinearities at Mach 0.9, 20,000 ft.

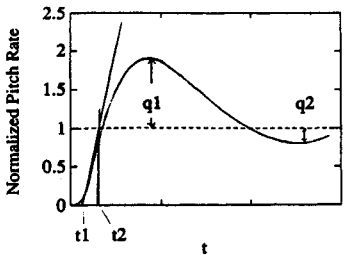

Fig. 2 Normalized pitch rate response criterion – effective time delay: $t_1 \leq 0.12$ s; transient peak ratio: $q_3/q_2 \leq 0.3$; effective rise time: 0.01 s $\leq t_2 - t_1 \leq 0.54$ s.

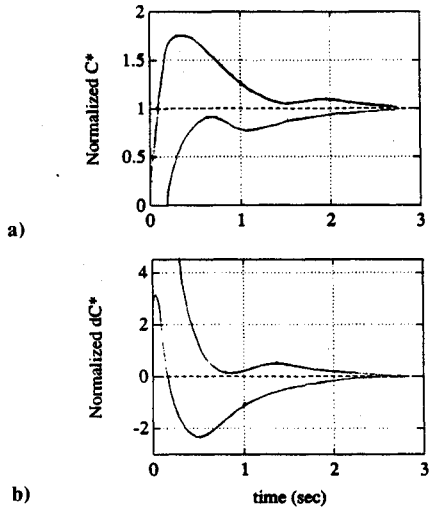

Fig. 3 Normalized C^*, dC^* response criterion.

$$A_{np} = A_{ncg} + l_x \dot{q}/g \tag{14}$$

where l_x is the distance of the pilot station from the center of gravity.

B. Performance Criteria

Various criteria have been developed with the idea of quantifying the flying qualities of the controller, as seen and felt by the pilot. Based on statistical research, criteria have been developed in both the time and frequency domain. In this study, time domain specifications are used.

The q Response Criterion

The response of the pitch rate q for a step input in the g command is specified by the initial response, the maximum delay, and the amount of oscillation from the steady state (see Fig. 2). Note that at the beginning, the response has a positive slope, that is, a nonminimum phase type of response would not be acceptable. Further, the limitations on the oscillations require that the system be well damped.

$C^*$and dC^* Response Criteria

C^* is by definition a particular linear combination of the incremental NLF at the pilot's location and the pitch rate. It has been found that if C^* satisfies a particular response requirement during a unit g command, the handling qualities are satisfactory to the pilots. Similarly, there is a requirement on the rate of change of C^* with respect to time dC^*

$$C^* \triangleq \Delta A_{np} + V_{c0} q/g$$

where ΔA_{np} is the incremental NLF at the pilot station and V_{c0} is defined to be 400 ft/s. Figures 3a and 3b show typical C^* and dC^* specifications.

III. Single Sliding Surface Design

Sliding controllers and nonlinear inversion have been discussed in great detail in the control literature (for example, see Fernandez and Hedricks[8] and Slotine[9]). In this paper the theory is applied to the aircraft model, and several modifications need to be made.

The output to be tracked is defined to be the NLF at the pilot station A_{np}. The inputs are the actuator commands for the elevator and the flaperon—u_{δ_e} and u_{δ_f}.

Differentiating the output once,

$$\dot{A}_{np} = f(\alpha, q, \theta) + \bar{w} + g_{\delta_e}(\alpha) u_{\delta_e} + g_{\delta_f}(\alpha) u_{\delta_f}$$

where $f(\alpha,q,\theta)$, $g_{\delta_e}(\alpha)$, and $g_{\delta_f}(\alpha)$ are nonlinear functions of the corresponding states. The $\bar{w}$ represents the lumped effect of the disturbances. To check for invertibility, write g_{δ_e} and g_{δ_f} explicitly:

$$g_{\delta_e}(\alpha) = 20\bar{q}S/q\left[(C_{l\delta_e}\cos\alpha + C_{d\delta_e}\sin\alpha) + l_x\bar{c}/I_{yy}C_{m\delta_e}\right]$$

$$g_{\delta_f}(\alpha) = 20\bar{q}S/q\left[(C_{l\delta_f}\cos\alpha + C_{d\delta_f}\sin\alpha) + l_x\bar{c}/I_{yy}C_{m\delta_f}\right]$$

For invertibility, $g_{\delta_e}(\alpha)$ and/or $g_{\delta_f}(\alpha)$ need to be nonzero. This condition can be written as

$$\sin(\phi_{\delta_e} + \alpha) \neq \frac{l_x\bar{c}m}{I_{yy}} \frac{C_{m\delta_e}}{\sqrt{C_{d\delta_e}^2 + C_{l\delta_e}^2}}$$

$$\sin(\phi_{\delta_f} + \alpha) \neq \frac{l_x\bar{c}m}{I_{yy}} \frac{C_{m\delta_f}}{\sqrt{C_{d\delta_f}^2 + C_{l\delta_f}^2}}$$

where $\tan\phi_{\delta_e} \triangleq C_{l\delta_e}/C_{d\delta_e}$ and $\tan\phi_{\delta_f} \triangleq C_{l\delta_f}/C_{d\delta_f}$. For the aircraft considered, the condition for the elevator is always satisfied, and is satisfied for the flaperon as long as $\alpha \neq 114$ deg or $\alpha \neq -111$ deg. Since such angles of attack are not meaningful, the system is always invertible.

To use the two inputs effectively, one can define $\bar{g}u_{\text{out}} \triangleq g_{\delta_e}(\alpha)u_{\delta_e} + g_{\delta_f}(\alpha)u_{\delta_f}$. Then

$$\dot{A}_{np} = f(\alpha, q, \theta) + g\, u_{\text{out}} + \bar{w}$$

where $g = 1$. The u_{out} is treated as the input, and one can proceed with inversion and sliding control. The sliding surface is defined as $S = A_{np} - A_{npd}$, and it is desired that $S \to 0$ independent of model errors and disturbances.

Differentiating S,

$$\dot{S} = \dot{A}_{np} - \dot{A}_{npd}$$

or,

$$\dot{S} = f - \dot{A}_{npd} + \bar{w} + \bar{g}u_{\text{out}}$$

Let the control be defined as

$$u_{\text{out}} = (\dot{A}_{npd} - \hat{f}(\alpha, q, \theta) - K\ \text{sgn}(S)/\hat{\bar{g}}$$

where $\hat{*}$ represents the estimate of the variable $*$, and K is chosen based on the bounds on the disturbances and model errors as follows.

Let the bounds be written as

$$|f - \hat{f} + \bar{w}| \leq \bar{w}_{\max}$$

$$|\bar{g}/\hat{\bar{g}} - 1| \leq \beta$$

with $\beta \leq 1$.

Then K is defined as

$$K = (\bar{w}_{\max} + \eta)/(1-\beta) + \beta/(1-\beta)(\dot{A}_{npd} - \hat{f})$$

It can be easily seen that with this control, $S\dot{S} \leq -\eta|S|$. Thus S reaches zero in finite time and on the average remains equal to

zero from then on, independent of the model errors and disturbances.

However, there is a lot of chattering in the input, and this directly gets reflected in the higher-order dynamics that have been neglected. Therefore a smoothing boundary layer[9] is employed. The new control law becomes

$$u_{\text{out}} = \left[\dot{A}_{npd} - \hat{f}(\alpha,q,\theta) - K\ \text{sat}(S/\phi)\right]/\bar{\hat{g}}$$

where sat(.) is the saturation function and ϕ is the boundary layer. Outside the boundary layer this ensures $S\dot{S} \leq -\eta|S|$, and thus the boundary layer is reached in finite time, and S stays inside the boundary layer from then on. The dynamics of S inside the boundary layer (for simplicity consider the case when $\beta = 1$, that is, there is no uncertainty on the term multiplying the input) is

$$\dot{S} = -KS/\phi + \left[(f - \hat{f}) + \bar{w}\right] \tag{15}$$

Thus, inside the boundary layer the dynamics on the sliding surface can be thought of as a first-order filter with bandwidth K/ϕ. Therefore, by appropriately choosing K/ϕ, the effect of chattering is eliminated, and the neglected higher-order dynamics are filtered.

The actual inputs are recovered from

$$u_{\delta_e} = u_{\text{out}}/g_{\delta_e}{}^*(1-\epsilon)$$

$$u_{\delta_f} = u_{\text{out}}/g_{\delta_f}{}^*\epsilon$$

where ϵ is a number from 0 through 1. The ϵ represents the relative use of the flaperon with respect to the elevator. The bound β can be obtained from the individual bounds on g_{δ_e} and g_{δ_f} as

$$\beta = \beta_{\delta_e}(1-\epsilon) + \beta_{\delta_f}\epsilon$$

A. Zerodynamics

The zerodynamics correspond to the dynamics of the unobservable part of the system when the output is held identically equal to zero (see, for example, Byrnes and Isidori[10]). Determining the zerodynamics usually involves a nonlinear coordinate transformation and analyzing the unobservable part of the transformed system under state feedback. It is well known that for a controller based on inversion to be feasible, the aerodynamics need to be stable; therefore the zerodynamics have to be checked for stability. It is important to note that "full state linearization"[2] defines a system that has no zerodynamics; however, finding such a transformation can be extremely difficult and the output of the linear system is generally a nonlinear function of the actual output. It is worthwhile to look at the zerodynamics of the linearized system because it not only provides information regarding the stability of the zerodynamics, but also a better idea of the entire system dynamics. The eigenvalues of the linearized zerodynamics are precisely the zeros of the transfer function of the linearized system.[12]

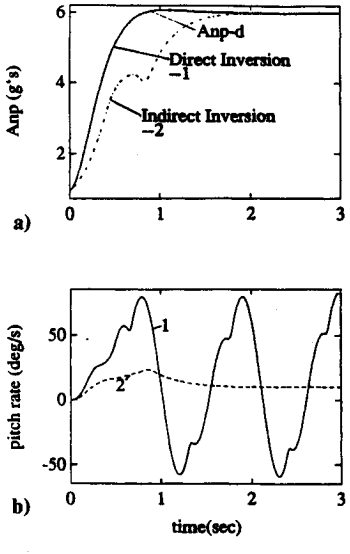

Fig. 4 Comparison of simulations of direct inversion and inversion through output redefinition – 6-g command.

Table 2 Transfer function zeros

Zero$_1$	Zero$_2$	ϵ
$-1.376 + 12.664i$	$-1.376 - 12.664i$	0
.	.	.
.	.	.
.	.	.
$-4.945 + 25.934i$	$-4.945 - 25.934i$	0.5
8.433	−8.109	1

Table 3 Transfer function zeros

Zero$_1$	Zero$_2$	ϵ	k_1	k_2
$-12.09 + 1.73i$	$-12.09 - 1.73i$	0.0	0.78	1.0
−41.93	−7.47	0.5	0.78	1.0
21.672	−5.279	1.0	0.78	1.0

Thus the zeros of the linearized system are calculated for various values of ϵ, the relative weighting factor of the elevator and the flaperon: there is a zero at the origin corresponding to $\dot{\theta} = q$. The other two depend on ϵ (see Table 2).

The zerodynamics are not acceptable for any ϵ because the specifications on the two variables C^* and q require considerable damping. That this is indeed true can be seen by considering the simulation of a 6-g pull-up in Fig. 4a—note the large oscillations in the pitch rate. The simulations are for $\epsilon = 0$.

Thus direct inversion is not a solution, and therefore a modified output approach is developed.

B. Modified Output

A modified output A^*_{np} is defined so that tracking A^*_{np} ensures acceptable zerodynamics by placing the zeros of the linearized system corresponding to the modified output. Then the reference trajectory for the modified output is chosen such that good tracking of the actual output is obtained, up to a definable set of frequencies.

Define A^*_{np} as

$$A^*_{np} = -k_1\dot{w}/g + qu/g + k_2\dot{q}l_x/q + \cos(\theta)$$

Note the following:

1) The preceding terms stand for the body frame acceleration, centripetal acceleration, the body frame angular acceleration, and the gravitational acceleration, relatively weighed by k_1, 1, k_2, and 1.

2) At steady state, $\dot{w} = 0$ and $\dot{q} = 0$, hence $A^*_{np} = A_{np}$.

3) When $k_1 = 1$ and $k_2 = 1$, $A^*_{np} = A_{np}$.

This modified output is closely related to the actual output. The zeros of the linearized system are given in Table 3. Notice that with decreased k_1, consistently better zeros are achieved except when the flaperons are used alone ($\epsilon = 1$). The actual choice of ϵ, k_1, k_2 is made based on 1) a tradeoff between α and δ_f (the flaperons saturate fast, but provide significant lift), and 2) the desired zeros. For the design, k_1 was chosen to be 0.78, and ϵ was varied based on the reference so as to strike a balance between the angle of attack and actuator saturation.

Physical Significance of the Modified Output

The modified output essentially demands more of the normal acceleration due to pitch rate (centripetal acceleration) as compared with the direct lift. This means that the controller

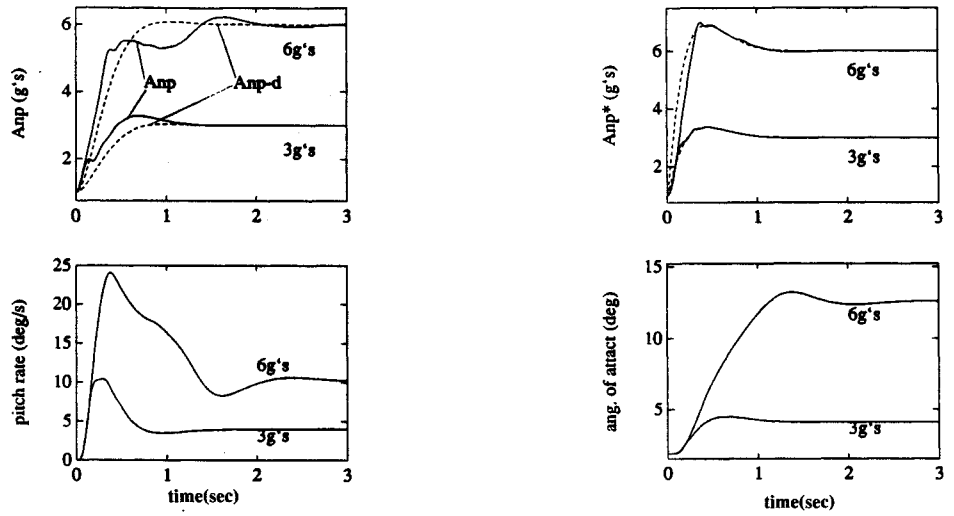

Fig. 5 Single sliding surface design – response of the output NLF, the pitch rate, and the angle of attack ($\epsilon = 0.081$ for 3 g)($\epsilon = 0.5$ for 6 g).

gives more importance to the moments created by the control surfaces as compared to the forces (lift) generated by them. This is interesting because it is a standard procedure in flight control (see for example, Lane and Stengel[3]) to neglect the forces created by the control surfaces, precisely for overcoming the troubles associated with the nonminimum phase character of the system.

A sliding controller is used to achieve $A^*_{np} = A^*_{npd}$. The details are omitted here because they parallel the procedure given in Sec. III.

Defining the Modified Desired Trajectory

The transfer function between A_{np} and A^*_{np} based on the linearized system is given by

$$A_{np} = \frac{N^u(s)N^a(s)}{N_m(s)} A^*_{np}$$

where $N^u(s)$ represents the undesirable zeros of the original output, $N^a(s)$ the acceptable zeros of the original output, and $N_m(s)$ the zeros of the modified output. During sliding,

$$A_{np} = \frac{N^u(s)N^a(s)}{N_m(s)} A^*_{npd}$$

Define

$$A^*_{npd} \triangleq \frac{N_m(s)N^+(s)}{N^a(s)} A_{npd}$$

then,

$$A_{np} = N^u(s)N^+(s)A_{npd}$$

It is a design issue to choose $N^+(s)$ so that good tracking is achieved at the frequencies of interest. One good way is to define $N^+(s) \triangleq N^u(-s)/[(N^u(0)]^2$ wherein zero phase error and near unity gain is ensured up to the frequencies determined by the undesirable zeros.

Figure 4 shows the improvement in the zerodynamics by using the modified output. The corresponding loss in performance of the actual output is minimal. Thus it is seen that very good pull-up maneuvers can be achieved by using this output redefinition approach. Section III.C discusses the numerical simulations obtained based on the complete model, including the higher order dynamics and saturation.

C. Simulations with Single Sliding Surface Design

The Mach number was assumed to be constant ($M = 0.9$) and the initial altitude for the 1-g trim condition was chosen to be 20,000 ft.

Figure 4 shows the need for not doing direct inversion and how, by redefining the output, good tracking and zerodynamics are obtained. For the simulations in Fig. 4, saturation was not considered. The reason is that if direct inversion is used, the pitch rate oscillates so much that it constantly saturates the actuator rates. In fact, this shows that another reason for requiring good zerodynamics is to limit the control authority.

It is assumed that the pilot stick force can be interpreted as a g command. The reference for the normal acceleration was obtained by passing the g command through a second-order filter whose characteristics are based on the specification for C^* and q.

Responses of the inputs and output, and the performance criterion variables for g commands of 3 and 6, are shown in Figs. 5–7. For the 3-g reference, ϵ was chosen to be 0.081. This in effect means using very little of the flaperons. The flaperons provide considerable lift. This implies that, for the same lift, more control authority is requested from the flaperon as compared to the elevator, and thus the flaperons quickly saturate. Therefore a small ϵ is chosen for a low reference such as 3 g so that the flaperons can still be used at further incremental commands.

For the 6-g reference, ϵ was chosen to be 0.5. Here one is forced to increase the relative use of the flaperon to prevent too high an angle of attack. As expected, more of the flaperons are used in this case (see Fig. 7) More important, the flaperon rate saturates (Fig. 7). This effect does not show up

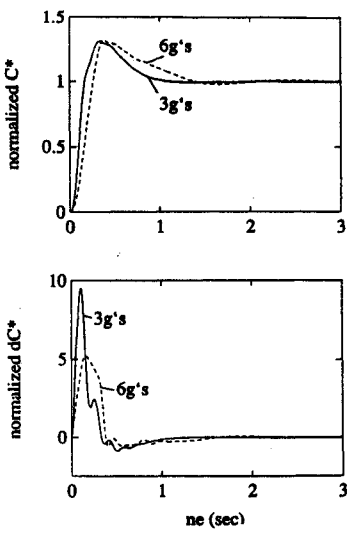

Fig. 6 Single sliding surface design – normalized response of C^* and dC^*.

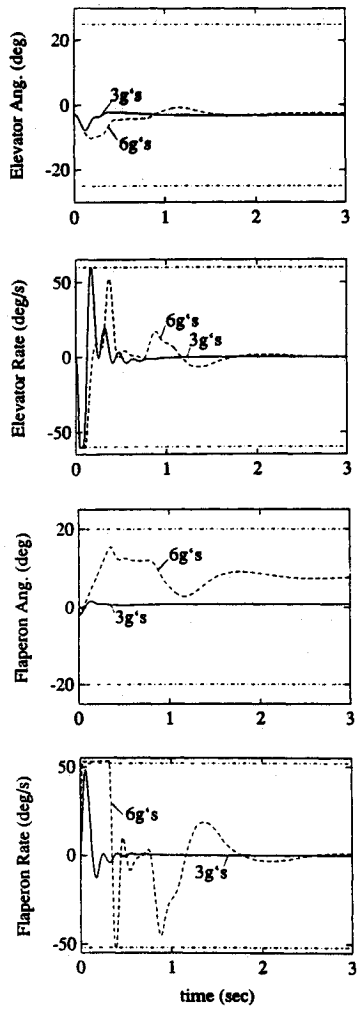

Fig. 7 Single sliding surface design – control authority – time histories of δ_e, δ_f, $\dot{\delta}_e$, and $\dot{\delta}_f$; the dash-dot lines show saturation limits.

in the actual output; however, a slightly wavy behavior of the pitch rate is seen (see Fig. 5). It is still within specifications at this 6-g reference and so are C^* and dC^* (see Fig. 6).

The performance of the output A_{np} (see Fig. 5) shows that the modified output approach works well, despite the fact that the modified reference trajectory was based on the linearized transfer functions. The small tracking errors in the transient (Fig. 5) are because of rate saturation in the elevator for the 3-g reference and rate saturation in the flaperon for the 6-g reference (Fig. 7), which are consequences of choosing the corresponding relative weights ϵ.

The simulations include the complete model: the actuator saturation and the higher-order dynamics. It is to be noted that neglecting the higher-order dynamics can be conveniently taken into account in the sliding controller design. In the present case, one needs to avoid frequencies above 52 rad/s. This can be done by limiting the bandwidth inside the boundary layer to less than 52 rad/s. The bandwidth inside the boundary layer is limited by K/ϕ [Eq. (15)]. Thus by setting $K/\phi \approx 40$ rad/s, one can ensure that the effect of the higher-order dynamics is negligible; however, the tradeoff is that one has more uncertainty, that is, if $w_{\max}$ is large, one is forced to have a bigger boundary-layer ϕ (larger tracking errors).

Figures 5-7 show that the performance of the sliding controller is very good. At higher g (around 9 g), actuator saturation becomes significant.

IV. Dual Sliding Surface Design

In Sec. III it was shown that the zerodynamics can be dictated to a large extent through output redefinition. This was necessary because of the given specifications on two independent variables while tracking a single output. One can do better than merely specifying the zerodynamics, noting that there are two inputs and that two specifications need to be specified. One can define the variables to be tracked as the specification variables, namely, C^* and q. The reference trajectories for these variables are defined so as to achieve the desired g pull up, while satisfying the specifications exactly (in the absence of saturation effects). This is a simple way of incorporating the specifications into the design phase itself.

Differentiating C^* once and q twice, the input/output relationship can be written as:

$$\begin{bmatrix} \dot{C}^* \\ \ddot{q} \end{bmatrix} = \begin{bmatrix} f_1(\alpha, q, \delta_e, \delta_f) + w_1 \\ f_2(\alpha, q, \delta_e, \delta_f) + w_2 \end{bmatrix} + \bar{J}(\alpha) \begin{bmatrix} u_{\delta_e} \\ u_{\delta_f} \end{bmatrix}$$

where $f_1(\alpha, q, \delta_e, \delta_f)$ and $f_2(\alpha, q, \delta_e, \delta_f)$ are nonlinear functions, and $\bar{J}(\alpha)$ is a matrix made of nonlinear functions as its elements. The w_1 and w_2 are the disturbances acting on the dynamics of each channel. This formulation of the disturbances assumes that matching conditions are satisfied by the disturbances.

For invertibility, $\bar{J}(\alpha)$ needs to be invertible. $\bar{J}(\alpha)$ can be written as

$$\bar{J}(\alpha) = \begin{bmatrix} g_{11} & g_{12} \\ g_{21} & g_{22} \end{bmatrix}$$

where

$$g_{11} = \left[\frac{\bar{q}S}{gm} (C_{l\delta_e} \cos\alpha + C_{d\delta_e} \sin\alpha) + \frac{\bar{q}S\bar{c}}{I_{yy}} \frac{lx}{g} C_{m\delta_e} \right] 20$$

$$g_{21} = 20 \frac{\bar{q}S\bar{c}}{I_{yy}} \frac{u}{g} C_{m\delta_e}$$

g_{21} and g_{22} are similarly defined.

It is necessary that

$$g_{11}g_{22} - g_{12}g_{21} \neq 0$$

After simplifying, it is required that

$$\left[C_{l\delta_e} C_{m\delta_f} - (C_{l\delta_f} C_{m\delta_e}) \right] \cos\alpha + \left[C_{d\delta_e} C_{m\delta_f} - (C_{d\delta_f} C_{m\delta_e}) \right] \sin\alpha \neq 0$$

The invertibility condition reduces to

$$\sin(\phi_{\text{inv}} + \alpha) \neq 0$$

where

$$\tan\phi_{\text{inv}} \triangleq \frac{(C_{l\delta_e}/C_{m\delta_e}) - (C_{l\delta_f}/C_{m\delta_f})}{(C_{d\delta_e}/C_{m\delta_e}) - (C_{d\delta_f}/C_{m\delta_f})}$$

One would like ϕ_{inv} to be as close to 90 deg as possible. For the aircraft considered, it is assumed that the coefficients with respect to the control surfaces are constant, and $\phi_{\text{inv}} = 88.7$ deg. Thus, again it is an invertible system.

There are two sliding surfaces of order 1 and 2, defined as follows:

$$S_1 = C^* - C_d^*$$

$$S_2 = (\dot{q} - \dot{q}_d) + \lambda_q (q - q_d)$$

One can consider the bounds on the model errors and the disturbances by dealing with the bounds on each component

of the model errors and disturbances as follows:

$$f_i = \hat{f}_i + \Delta f_i$$

$$\bar{w}_i = \hat{\bar{w}}_i + \Delta \bar{w}_i$$

$$\bar{J} = \hat{\bar{J}}(I + \delta \bar{J})$$

for $i = 1,2$. Let

$$|\Delta f_i| \le \alpha_{fi}$$

$$|\Delta \bar{w}_i| \le \alpha_{wi}$$

$$|g_{jk}| \le \beta_{jk}$$

for $i, j, k = 1,2$. For invertibility, it is necessary that $\|\delta \bar{J}\| < 1$ (see the Appendix for details).

Proceeding with inversion, and by including sliding gains, the following control is obtained:

$$\begin{bmatrix} u_{\delta_e} \\ u_{\delta_f} \end{bmatrix} = \bar{J}^{-1}(\alpha) \begin{bmatrix} \dot{C}_d^* - f_1(\alpha, q, \delta_e, \delta_f) - (k_1)\ \mathrm{sgn}(S_1) \\ \ddot{q}_d - \lambda_q(\dot{q} - \dot{q}_d - f_2(\alpha, q, \delta_e, \delta_f) - (k_2)\ \mathrm{sgn}(S_2) \end{bmatrix} \tag{16}$$

The sliding gains k_1 and k_2 are chosen as follows:

$$\begin{pmatrix} k_1 \\ k_2 \end{pmatrix} = \left(I - B\right)^{-1} \left\{ \begin{pmatrix} \alpha_{f1} + \alpha_{w1} + \eta_1 \\ \alpha_{f2} + \alpha_{w2} + \eta_2 \end{pmatrix} + B \begin{pmatrix} |\hat{f}_1| \\ |\hat{f}_2| \end{pmatrix} \right\} \tag{17}$$

where B is the matrix $\{\beta_{ij}\}$, $i,j = 1,2$.

This control ensures that (see the Appendix for the proof)

$$S_1 \dot{S}_1 \le \eta_1 |S_1|$$

$$S_2 \dot{S}_2 \le \eta_2 |S_2|$$

On the average, this ensures (without saturation)

$$S_{1\mathrm{av}}, \dot{S}_{1\mathrm{av}} = 0$$

$$S_{2\mathrm{av}}, \dot{S}_{2\mathrm{av}} = 0$$

and $C^* = C_d^*$ and $(\dot{q} - \dot{q}_d) + \lambda_q(q - q_d) = 0$.

To prevent the high chatter associated with the preceding control, replace the sign function with the saturation function as in the single sliding surface design.

A. Desired Trajectories

It is necessary to design trajectories so that $A_{np} \to g_{\mathrm{command}}$ at steady state. At steady state $A_{np}|_{ss} = qu/g + \cos(\theta)$. Thus,

$$q_{dss} = \left[g_{\mathrm{command}} - \cos(\theta)\right] g/u$$

$$C_{dss}^* = (V_{c_0} + u)/u \left[g_{\mathrm{command}} - \cos(\theta)\right]$$

Set

$$q_d = \frac{\omega_{qd}^2}{s^2 + 2\xi_q \omega_q s + \omega_{qd}^2} q_{dss}$$

$$C_d^* = \frac{\omega_{C_d^*}^2}{s^2 + 2\xi_{C_d^*} \omega_{C_d^*} s + \omega_{C_d^*}^2} C_{dss}^*$$

where ω_{qd}, ξ_{qd}, $\omega_{C_d^*}$, and $\xi_{C_d^*}$ are chosen based on the specifications given for q and C^*. Thus, specifications are satisfied exactly while achieving the desired g pull up.

The zerodynamics need to be stable, and in this case the linearized zeros are -0.092 and 0. If the dynamics of the system are observed, one notes that the zero at the origin comes from the presence of the dynamic relation $\dot{\theta} = q$ [Eq. (3)]. The only way θ enters the dynamics of the other variables is in $\dot{w}$ [Eq. (1)] through a $\cos(\theta)$ term, which is bounded for all values of θ. Thus one can consider $\cos(\theta)$ as a bounded disturbance term and proceed with the same analysis as before and arrive at the conclusion that the system excluding θ is indeed stable—the eigenvalue corresponding to the zerodynamics would be at -0.092. In particular, for bounded references, all the state variables will be bounded.

Apart from having to be stable, the zerodynamics does not need to have any special characteristics (like low damping, etc.) because all the specifications have been satisfied.

In Sec. IV.A, the simulations show that this dual surface design leads to a superior controller.

B. Simulations with Dual Sliding Surface Design

The same model was used as in the single sliding surface case. The only change was in the controller.

Figures 8 and 9 show the performance for the same 3- and 6-g commands. Notice that the performance is significantly better in that the controller is smoother while the specifications are satisfied exactly.

In Fig. 8, corresponding to a 3-g reference, note that the response of the output A_{np} "tracks" the desired trajectory for the output A_{np} (a linear combination of the desired trajectories of C^* and q). Thus the specifications are satisfied completely. One can also see that the control surfaces and their rates do not saturate (see Fig. 9).

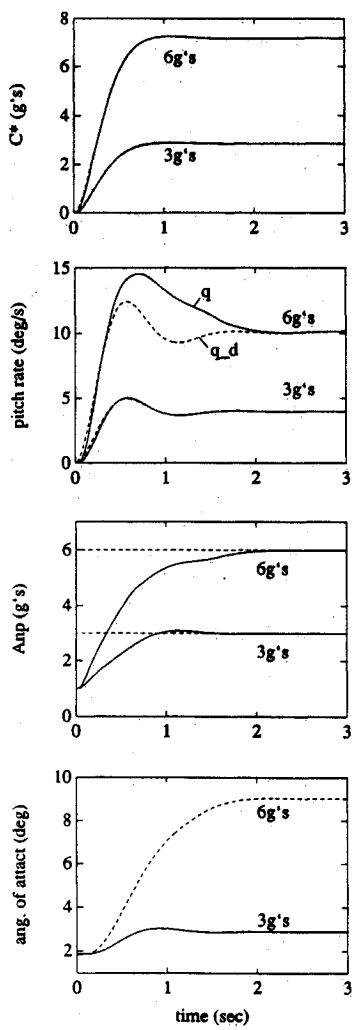

Fig. 8 Dual sliding surface design – response of the NLF, the "outputs" C^* and q, and the angle of attack for 3- and 6-g commands.

Notice that the flaperon used (~9.5 deg) in this dual surface design is higher than the flaperon (~0.75 deg) in the previous approach (Fig. 7). This is because the previous approach specifies how much of the flaperons are to be used without actually looking at the dynamics of the pitch rate, whereas here no restrictions on the flaperons are imposed other than a desired pitch rate.

For the 6-g reference, note that perfect tracking of C^* is attained, but only good tracking of the pitch rate. The reason for this is saturation of the controls (see Fig. 9). The flaperon rate saturates at the start, and that manifests itself as a tracking error. In spite of the saturation, the performance specifications are satisfied.

Figure 10 shows the effect of model error and the use of sliding control to eliminate it. The dotted lines show the performance of the input/output linearization approach, whereas the solid line shows that of the sliding approach. Notice that a 10% error in the aerodynamic coefficients in the controller results in a definitely undesirable performance if input/output linearization is attempted alone, while sliding control takes care of it and makes the performance robust to such model errors and disturbances. It is important to note in this context that sliding control is a special case of input/output linearization; i.e., sliding control has additional terms that keep the output close to the desired surface.

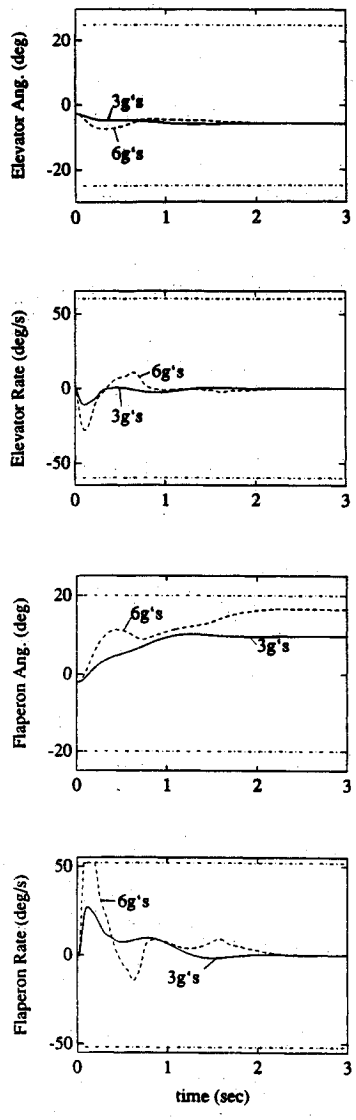

Fig. 9 Dual sliding surface design – control authority – time histories of δ_e, δ_f, $\dot{\delta}_e$, and $\dot{\delta}_f$. The dash-dot lines show saturation limits.

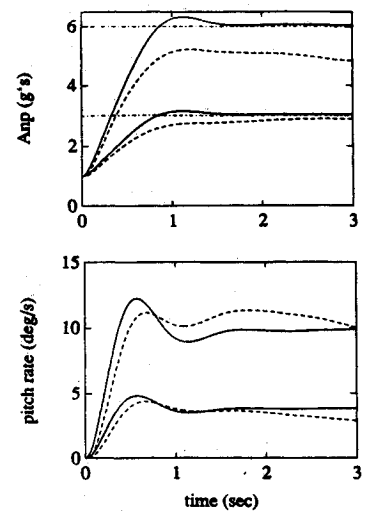

Fig. 10 Robustness of sliding controller to model errors – response of the dual sliding surface controller vs the dual surface linearizing controller in the presence of a 10% error in each of the following aerodynamic coefficients: $C_{l\alpha}$, C_{lq}, $C_{m\alpha}$, and C_{mq}.

V. Conclusions

This paper has investigated the use of sliding controller design for high-performance aircraft that can have significant nonlinear dynamic behavior. Sliding control is essentially an input/output linearization method with additional terms that account for model errors. Since the resulting dynamics are "nearly linear," it is a straightforward procedure to incorporate performance specifications that are based on linear response, either in the time or frequency domain. The method of generating a desired reference trajectory that meets flying quality specifications is similar to a model following approach, although it is important to note that a dynamic model of the aircraft has not been used, but rather a simple second-order, open-loop system to accept the pilots "step" g command and to generate C^* and q trajectories that satisfy flying quality specifications.

It has been assumed that all disturbances lie in the space spanned by the control vectors; if not, the bounds on their time rates of change must be estimated to guarantee robustness.

Two approaches were developed in this paper for a pitch-plane flight controller. In the first approach, better zerodynamics is achieved by output redefinition. A modified output was defined that has minimum phase zeros and tracks the original output at low frequencies.

In the second approach, two inputs are used independently, and by defining the specification variables as the variables to be tracked, one can incorporate the specifications directly into the design stage.

Though saturation is not seen to be important up to around 7 g, it does become important from then on and significantly alters the performance around 9 g. An important consideration in the future will be to design trajectories that have minimal saturation. Adaptive controllers will also be included in the future so that one can reduce unnecessary control authority and thereby reduce saturation.

Appendix: Sliding Controller Robustness for the Multi-Input/Multi-Output Systems

An expression is derived for choosing the sliding gains for a multi-input/multi-output system such that the system dynamics reach the sliding surface in finite time and stay there from then on. This has been worked out so far only for single-input/single-output systems.

The dynamics on the sliding surfaces can be written as

$$\dot{S} = f + \bar{w} + \bar{J}u \qquad \text{(A1)}$$

where f is the $n \times 1$ vector whose elements are a nonlinear function of the states, the desired trajectory, and its derivatives; $\bar{w}$ is the $n \times 1$ vector representing external disturbances, J is the $n \times n$ invertibility matrix, and u is the $m \times 1$ vector of inputs. This formulation assumes the matching condition on the disturbances: If the plant dynamics can be written as

$$\dot{x} = f^*(x) + g^*(x)u + \bar{v}$$

where x is the state vector, $f^*(.)$, and $g^*(.)$ are nonlinear functions of the state, u the input vector, and v the effect of the disturbances and the model errors, $\bar{v}$ should satisfy

$$\bar{v} = g^*(x)\bar{w}$$

Let the control be

$$u = -\hat{J}^{-1}(\hat{f} + \hat{\bar{w}} + K\mathbf{1}_S) \tag{A2}$$

where $\hat{*}$ represents the estimate of the variable $*$. $K = \text{diag}\,(k_1, k_2, \ldots, k_n)$, $k_i \geq 0$ for $i = 1, \ldots, n$, and $\mathbf{1}_S$ is defined by

$$\mathbf{1}_S \triangleq \begin{bmatrix} S_1/|S_1| \\ S_2/|S_2| \\ \cdot \\ \cdot \\ \cdot \\ S_n/|S_n| \end{bmatrix}$$

One can find k_i so that the desired robustness properties are obtained. With the control as in Eq. (19),

$$\dot{S} = f - J\hat{J}\hat{f} - J\hat{J}\mathbf{1}_S \tag{A3}$$

Let the estimates be related to the actual variables as follows:

$$f = \hat{f} + \Delta f$$

$$\bar{w} = \hat{\bar{w}} + \Delta\bar{w}$$

$$J = (I + \delta J)\hat{J}$$

where $\delta J = \{\delta J_{ij}\}$, $i, j = 1, \ldots, n$. Let the bounds be given by

$$|\Delta\bar{w}_i| \leq \alpha_{wi}$$

$$|\Delta f_i| \leq \alpha_{fi}$$

$$|\delta J_{ij}| \leq \beta_{ij}$$

$i, j = 1, \ldots, n$. Define the matrix formed by β_{ij} as B and the maximum singular value of B to be β. Using maximum singular value norms for matrices, one has

$$\beta \leq \max \|\delta J\| \tag{A4}$$

It is assumed that one has sufficient knowledge of the system, that whenever $\hat{J}$ is invertible J is also invertible. This implies that $I + \delta J$ is invertible and

$$1 = \sigma_{\min}(I) > \sigma_{\max}(\delta J) = \|\delta J\|$$

for all δJ. This implies, from Eq. (21),

$$\beta = \|B\| < 1 \tag{A5}$$

Substituting the preceding relations in $\dot{S}$

$$\dot{S} = \Delta f + \Delta\bar{w} - \delta J\hat{f} - (I + \delta J)K\mathbf{1}_S$$

Premultiplying by S^T and taking components

$$S_i\dot{S}_i = S_i(\Delta f_i + \Delta\bar{w}_i) - S_i\sum_{j=1}^{n}\delta J_{ij}\hat{f}_j - |S_i|k_i - |S_i|k_i\delta J_{ii} - S_i\sum_{j=1\neq i}^{n}k_j\delta J_{ij}S_j/|S_j|$$

Or,

$$S_i\dot{S}_i \leq |S_i|(\alpha_{fi} + \alpha_{wi} + \sum_{j=1}^{n}\beta_{ij}|\hat{f}_j| + \sum_{j=1\neq i}^{n}B_{ij}k_j - k_i(1-\beta_{ii})$$

Therefore, one can choose

$$k_i(1-\beta_{ii}) - \sum_{j=1\neq i}^{n}\beta_{ij}kj = \alpha_{fi} + \alpha_{wi} + \sum_{j=1}^{n}\beta_{ij}|\hat{f}_j| + \eta_i \tag{A6}$$

so that

$$S_i\dot{S} \leq \eta_i|S_i| \tag{A7}$$

for $i = 1, \ldots, n$. Writing it concisely, it is sufficient that

$$(I - B)K = \gamma$$

where $K = [k_1, \ldots, k_n]^T$, and as γ is the vector whose ith element is given by

$$\alpha_{fi} + \alpha_{wi} + \sum_{j=1}^{n}\beta_{ij}|\hat{f}j| + \eta_i$$

Now, $(I - B)$ is nonsingular because $1 = \sigma_{\min}(I) > \sigma_{\max}(B) = \beta$. Thus choosing the sliding gains from

$$K = (I - B)^{-1}\gamma \tag{A8}$$

Eq. (23) is achieved, and therefore Eq. (24) is satisfied.

References

[1]Garrard, W. L., and Jordan, J. M., "Design of Nonlinear Automatic Flight Control System," *Automatica,* Vol. 13, 1977, pp. 497–505.

[2]Meyer, G., Sui, R., and Hunt, L. R., "Application of Nonlinear Transformations to Automatic Flight Control," *Automatica,* Vol. 20, Jan. 1984, pp. 103–107.

[3]Lane, S. H., and Stengel, R. F., "Flight Control Design Using Nonlinear Inverse Dynamics," *Automatica,* Vol. 24, 1988, pp. 471–483.

[4]Elgersma, N., and Morton, B., "Partial Inversion of Noninvertible Nonlinear Aircraft Models," UCB-NASA Ames Nonlinear Flight Control Workshop, Univ. of California, Berkeley, Aug. 1989.

[5]Hauser, J., Sastry, D., and Meyer, G., "Nonlinear Controller Design for Flight Control Systems," Memo UCB/ERL M88/76, Dec. 1988.

[6]Kapasouris, P., Athens, M., and Stein, G., "Design of Feedback Control Systems for Unstable Plants with Saturating Actuators," *IFAC Symposium on Nonlinear Control Systems Design*, edited by A. Isidori, IFAC, Capri, Italy, June 1989, pp. 302–307.

[7]White, B. A., Mudge, S., Patton, R. J., and Aslin, P. P., "Reduced Order Variable Structure Control of the Lateral Motion of an Aircraft," 25th CDC, Athens, Greece, Dec. 1986.

[8]Fernandez, B., and Hedrick, J. K., "Control of Multivariable Nonlinear Systems by the Sliding Mode," *International Journal of Control*, Vol. 46, Sept. 1987, pp. 1019–1040.

[9]Slotine, J. J., "Sliding Controller Design for Nonlinear Systems," *International Journal of Control*, Vol. 40, 1984, p. 421.

[10]Byrnes, C., and Isidori, A., "The Analysis and Design of Nonlinear Feedback Systems, Part I: Zero Dynamics and Global Normal Forms," *Nonlinear Control and Robotics,* Dipartimento di Informatica e Sistematica, Universita di Roma, 'La Sapienza,' 1988.

[11]Garrard, W. L., Enns, D. F., and Snell, A., "Nonlinear Longitudinal Control of a Supermaneuverable Aircraft," *Proceedings of the 1989 Automatic Control Conference*, pp. 142–147.

[12]Verghese, G. C., Fernandez, B. and Hedrick, J. K., "Stable, Robust Tracking by Sliding Mode Control," *Systems and Control Letters*, Vol. 10, 1988, pp. 27–34.